Characterisation of thin solid Xe targets

Article *in* Journal of Radioanalytical and Nuclear Chemistry · February 2014

DOI: 10.1007/s10967-013-2622-8

7 authors, including:

N. Y. Kheswa

26 PUBLICATIONS **99** CITATIONS

SEE PROFILE

Carlos Pineda-Vargas

iThemba Labs - Laboratory for Accelerator Based Science

76 PUBLICATIONS **309** CITATIONS

SEE PROFILE

Wojciech J Przybyłowicz

AGH University of Science and Technology in Kraków

199 PUBLICATIONS **3,122** CITATIONS

SEE PROFILE

Tshifhiwa Elmon Madiba

National Metrology Institute of South Africa

17 PUBLICATIONS **163** CITATIONS

SEE PROFILE

Characterisation of thin solid Xe targets

N. Y. Kheswa, P. Papka, C. Pineda-Vargas, W. J. Przybylowicz, G. F. Steyn, T. E. Madiba & J. F. Sharpey-Shafer

Journal of Radioanalytical and Nuclear Chemistry
An International Journal Dealing with All Aspects and Applications of Nuclear Chemistry

ISSN 0236-5731
Volume 299
Number 2

J Radioanal Nucl Chem (2014)
299:1067-1072
DOI 10.1007/s10967-013-2622-8

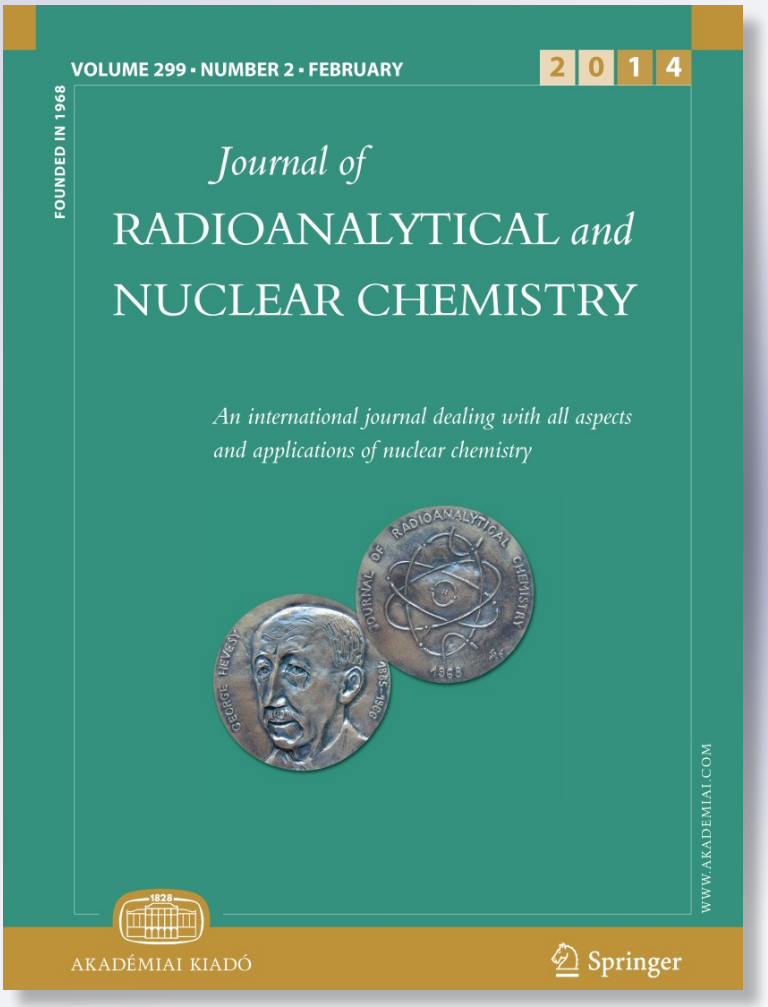

Springer

J Radioanal Nucl Chem (2014) 299:1067–1072
DOI 10.1007/s10967-013-2622-8

Characterisation of thin solid Xe targets

N. Y. Kheswa · P. Papka · C. Pineda-Vargas · W. J. Przybylowicz · G. F. Steyn · T. E. Madiba · J. F. Sharpey-Shafer

Received: 26 June 2013 / Published online: 18 July 2013

Abstract A series of frozen xenon targets of thicknesses ranging between 1 and 15 mg/cm^2 were characterised by elastic backscattering technique using a 3 MeV proton beam. Xenon was kept solid on a gold substrate having a thickness of 1 g/cm^2 which was mounted on a cold copper finger. The temperature of targets during the experiment was maintained at 55 K by a compact solid nitrogen sublimation system under pressure of 10^{-5} mbar. Targets were used in series of experiments for populating samarium and gadolinium isotopes in the ^{136}Xe (^{18}O, Xn) and ^{136}Xe (^{22}Ne, Xn) nuclear reactions.

Keywords Xenon targets · EBS · Characterisation · Frozen targets · Thickness · Gold backing

N. Y. Kheswa (✉) · C. Pineda-Vargas · W. J. Przybylowicz · G. F. Steyn
iThemba LABS, P.O. Box 722, Somerset West 7129, South Africa
e-mail: Kheswa@tlabs.ac.za

P. Papka
Department of Physics, University of Stellenbosch, Private Bag X1, Matieland 7602, South Africa

C. Pineda-Vargas
Faculty of Health and Wellness Sciences, CPUT, PO Box 1906, Bellville 7535, South Africa

W. J. Przybylowicz
Faculty of Physics and Applied Computer Science, AGH University of Science and Technology, Al. A. Mickiewicza 30, 03-059 Kraków, Poland

T. E. Madiba · J. F. Sharpey-Shafer
Department of Physics, University of Western Cape, Private Bag X17, Bellville 7535, South Africa

Introduction

In the literature, a number of measurements are reported where Xe target material is contained within thin windows of a gas cell at a pressure of about 1 bar [1]. Mostly such targets were dealt with in intermediate energy physics or production of heavy and super heavy elements. Only one thin solid xenon target has been reported for similar purposes to our experimental investigation in [2, 3] and more details on this target can be found in [4] and references therein. The solid Xe targets in this case were chosen instead of gas cell targets to avoid low—Z contaminants and to keep the γ-ray emitters at the centre point which is desired when using Compton escape-shielded detectors fitted with collimators of a reaction chamber. In γ-ray spectroscopy, the background originating from Compton Scattering is the major limiting factor; therefore contamination from parasitic nuclear reactions should be avoided. Gas cells are attractive but the windows, though made of thin film material, are likely to contain unwanted contaminants. Typically, windows are made of Havar (Co, Cr, Ni and traces of other elements including W), polymers such as Aramid or Kapton (H, C, N, O) also thin TA windows, $Z = 73$ are widely used. The windows of the gas target used in [1] had a thickness of 2.0 mg/cm^2 films of Ti, compared to that of a target just less than 3.0 mg/cm^2 of Xe. Such target makes γ-ray spectroscopy very challenging because of the large reaction rate on Ti nuclei [1].

The cryogenic targets described in this paper were developed for a set of γ-ray spectroscopy experiments with the AFRODITE γ-ray spectrometer of iThemba LABS, Cape Town, an arrangement of nine Clover detectors and eight Low Energy Photon Spectrometer germanium detectors [5]. Regarding Doppler broadening, two strategies can be adopted depending on the life-time of the γ-ray

emitters. Firstly, if the states are very short-lived, sub ps, it is advisable not to stop the recoils and perform the correction of the Doppler shift assuming that the evaporation residues do not deviate from the beam axis. If the characteristic life-time of the states of interest is long enough, greater than a few ps, the recoils are preferably stopped before γ-ray emission occurs. In the last instance, appropriate backing on a target for recoil stopping should be chosen so that the incident ion beam would strike below the Coulomb barrier on the backing material. Coulomb excitation events originating from the backing and characterised by low-multiplicity γ-ray emission are subsequently filtered with a trigger level of the γ-ray spectrometer greater than 1 γ-ray in coincidence. Gold and bismuth materials were used for target characterization and for nuclear physics measurements as a stopping material for the evaporation residues. The incident beam energy was lower than the Coulomb barrier on both Au and Bi.

Experimental set up

Cryogenic Xe target

The freezing point of Xe is 165 K at atmospheric pressure but owing to its high vapor pressure, the loss of target material via sublimation under vacuum is dramatic if the temperature is not substantially reduced. Consequently, at the pressure required for ion beam transport of $\approx 10^{-5}$ mbar, the temperature should be maintained below 60 K. In this work, the temperature was kept at 55 K with the use of the set up displayed in Fig. 1. The set up comprises of a Dewar flask filled with 3 l of liquid nitrogen (LN_2) with a holding time of 36 h. The atmosphere surrounding LN_2 was evacuated with a rotary pump through the inlet pipe (see bottom part of Fig. 1) to a pressure of less than 10^{-1} mbar. A copper finger of 220 mm length and 20 mm in diameter was bolted to the aluminium inner tank of the Dewar for holding a target with and the thermal conducting grease used to fill the interstices and improve the thermal contact between the two materials. The tip of the copper finger was adequately shaped in order to ensure minimum shadowing of the detectors. A gold substrate with areal density of 1 g/cm^2 was attached to the cold finger and good thermal contact was ensured with indium wire pressed between the gold substrate and the copper finger. The multi-layered insulation between the inner and outer tanks of the Dewar vessel was evacuated through the reaction chamber with the pumping system of the beam line.

The temperature of the target system was continuously monitored with a PT100, a temperature sensitive resistor which was attached on the tip of the cold finger. During the experiment, a 60 mm diameter thermal shield made of a

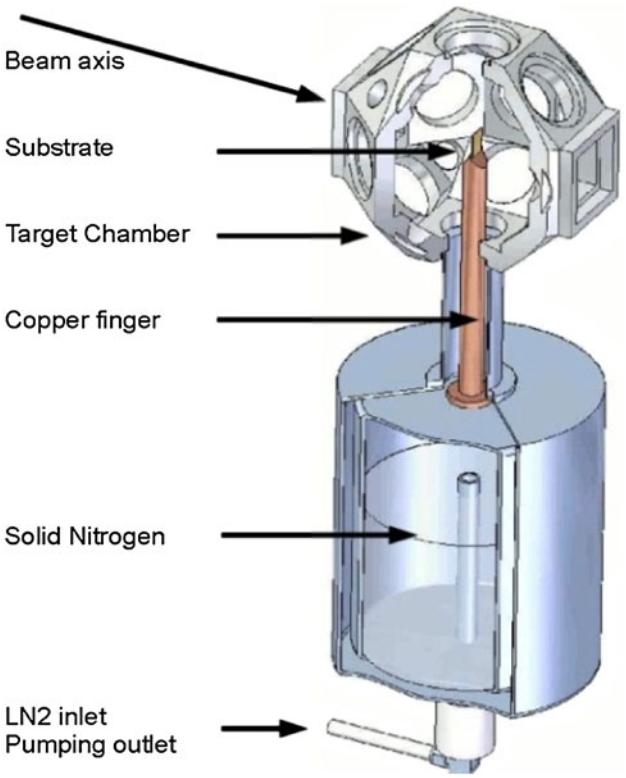

Fig. 1 Schematic view of the frozen nitrogen cryogenic target

2 mm diameter copper wire wrapped with a thin aluminium foil was placed at the tip of the cold finger to encapsulate the gold substrate. The shield had two holes covered with thin transparent plastic in order to monitor the beam visually observing the phosphorescence of Xe under irradiation and to insert a retractable Xe gas feeder. Another function of the shield was to maintain a clean vacuum by trapping the bulk of water and oil so they can be prevented from depositing on the cold substrate. However, no major difference was observed in the loss of Xe material with and without the thermal shield.

Every 36 h the Dewar had to be vented with gaseous nitrogen and recycled thermally as the minimum temperature tends to increase with time. This temperature change was suspected to arise from water and oil pollution of the insulating layers of the Dewar which is believed to cause loss of insulation inducing a few degree increase of the minimum temperature. The thermal recycling was achieved by heating the inner part of the Dewar with a thermistor. Then the Dewar was refilled with LN_2 and the temperature decrease again was obtained by means of evaporation under vacuum until the freezing occurred at 63 K, 14° below the boiling point. Note that the cooling of a 3 l volume of LN_2 down to the freezing point is rather quick, it takes approximately half an hour as the mixing of colder and warmer nitrogen through convection is very efficient. The temperature stabilizes at 64 K for a short while during the phase transition. Whereas,

cooling under sublimation is a slower process as it relies on the heat conduction through solid nitrogen which is a poor conductor of heat. The temperature curve during freezing is shown in Fig. 2. After freezing of LN_2 the temperature drops by another 6° through sublimation in about 1 h. The whole cooling down process from room temperature takes 2 h.

For the experiment ^{136}Xe with an enrichment of 99.8 % was applied. The enriched ^{136}Xe was introduced to the centre of the substrate with a retractable gas feeder connected to the bottle holding the enriched material. The feeder had two (a quarter turn and leak a low rate) valves connected in series, in which a volume of approximately 2 cm^3 was kept in between the valves. This amount of 2 cm^3 gas volume at 1 bar pressure was evacuated through a leak valve in order to control the rate of Xe depositing on the substrate. This process was repeated every 8 h to compensate for the loss of the xenon material.

During the method development gold and bismuth were tried as substrate material. In the end gold was chosen because of its good thermal conduction and its high atomic number. The thermal properties of gold allowed the use of high beam intensity compared to bismuth where the beam current had to be reduced to prevent rapid loss of target material. The differences in densities of Au and Bi are found to be 19.7 and 10 g/cm^2, respectively in which the stopping time of the recoils also differs substantially. Tests were performed with a layer of 30 mg/cm^2 Bi deposited on the gold substrate. Bismuth is used in nuclear physics experiments because when it comes to contaminating Coulomb excitation reactions, it gives much lesser γ rays than gold. Also the stopping time differs from that of gold resulting in some advantage for life-time measurement of nuclear excited states. Even though Xe froze during the trials the beam intensities had to be reduced to prevent a rapid loss of the material. Finally, the target consisted of a Au backing of 1 g/cm^2 ($\approx$0.52 mm) thickness, mounted onto a Cu cold finger cooled by LN_2 with a thin layer of frozen Xe onto the free surface of the Au backing. The Au backing had a rectangular shape with 16 mm in width and 18 mm in height. Two Xe thicknesses were considered, 1.5 mg/cm^2 ($\approx$4.1 μm) and 15 mg/cm^2 ($\approx$41 μm). A PT100 resistor mounted on the bottom edge of the target (at the interface between the Au and the cold finger) confirmed that the temperature on that boundary was kept constant at a value of 55 K. A thin Indium packing insures good thermal coupling at the Cu/Au interface and the thermal contact resistance is assumed (with a good measure of confidence) to be negligible.

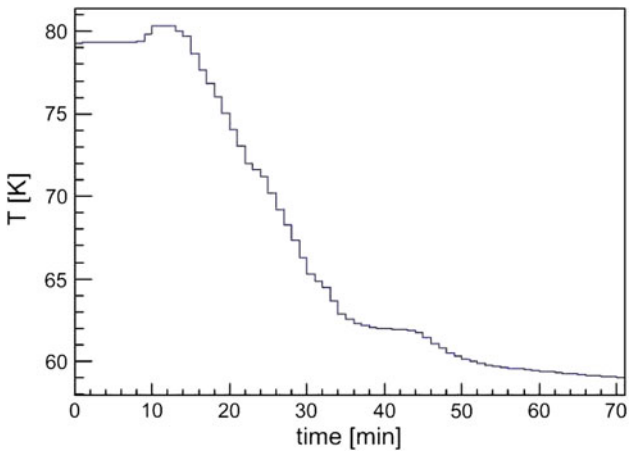

Fig. 2 Temperature curve at the tip of the copper finger, clearly showing the phase transition of the nitrogen from liquid to solid

Target characterisation

A number of targets with thicknesses ranging between 1 and 15 mg/cm^2 were prepared and characterized. However, only one target with a thickness of 1 mg/cm^2 will be described in detail in this work. Also targets with thicknesses greater than 15 mg/cm^2 were produced but could not be characterised with this method as the proton beam energy was not sufficient to reach the gold substrate and penetrate out of the Xe layer.

The characterisation of targets was performed by means of EBS using an $E_{\mathrm{lab}} = 3$ MeV proton beam of 2 mm diameter spot size. A useful feature of the Xe target is the phosphorescent emission spectrum within the visible range under ion beam irradiation, making beam monitoring possible with a camera pointing at the target while the measurement itself is performed. A surface barrier silicon detector was placed at an angle $\theta = 135°$ ($\Omega = 1.67$ msr) and the target was scanned over a mesh of 2 mm step size on a total surface area of 100 mm^2. It should be noted that the characterisation was performed without a thermal shield which resulted in a contamination on the surface of the target of oxygen and carbon. This was done since deposition rate was not initially known and the shield was meant to keep the rate low for nuclear physics experiment. At the time of the characterization it was easier to run without the shield (for RBS), it turns out we should actually have made two measurements to see how the shield improves the situation. Figure 3 shows the peaks resulting from interstitial contamination which occurred between the cooling of the cold finger and the deposition of Xe.

Calculations

Two well-focused beams (approximately 2 mm in diameter) have been used, namely 69 MeV ^{18}O and 90 MeV ^{22}Ne. The beam current typically did not exceed 10^{10} ions/s. The worst case, from a thermal heating point of view, would have been the Ne beam at a current of 10^{10} ions/s with a

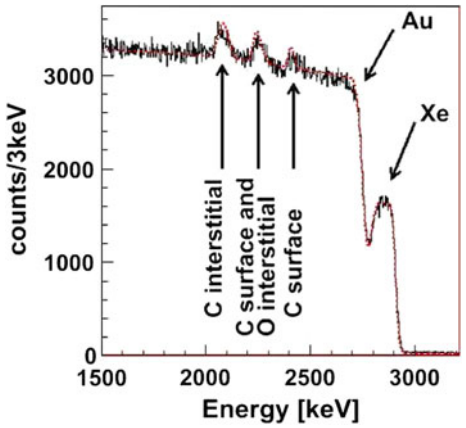

Fig. 3 EBS spectrum obtained from the bombardment with a 3 MeV proton beam of a thin Xe target deposited on a gold substrate. The peaks from the interstitial and surface O/C contamination are indicated with *arrows*. The fit (*dashed* was performed with SIMNRA [6])

thermal load of $Q = 90$ mW thus this case is considered first. Some relevant physical properties of Au and solid Xe are given in Table 1. In the temperature region 50–100 K, the temperature dependence of the thermal conductivity of Au and Xe is almost negligible and constant values have been adopted. It is instructive to first consider two hypothetical cases, which will help to justify a few approximations which will be introduced into the thermal model shortly.

Case 1

The Au backing on its own is considered. The thermal load equivalent to the heat dissipated by the Ne beam is incident from above onto the "thin" top surface of the target. From Fourier's law of heat conduction, it is a simple matter to calculate that for the case where $T_0 = 55$ K, the temperature at the top would be $T_1 = 55.53$ K. The temperature increase is less than 1 K, thus it is clear that 90 mW will not significantly heat such a thick Au substrate with excellent thermal conductivity.

Case 2

The Au backing on its own is considered. An axial symmetry around the beam direction is adopted, such that the temperature near the edge of the Au substrate is assumed to be constant. Such an approximation is justified, considering that it has already been shown in "Case 1" that the beam will not significantly heat the Au substrate. If one now assumes that the beam has a diameter of 3 mm and a uniform radial profile, one can again use Fourier's law to calculate the temperature difference across the target thickness. One finds a value of $\Delta T = 0.02$ K. Thus, one can ignore any axial temperature differences in the Au backing and consider only conduction in a radial direction to calculate a radial temperature profile. This is done for two beams, namely (1) a beam with a uniform profile, and (2) a beam with a Gaussian profile, truncated and renormalized so that it has a width of 2× FWHM = 3 mm. A finite differences approach similar to that in [6] is used. For a constant temperature of $T_0 = 55$ K at a radius of 8 mm from the centre of the beam, one obtains the following maximum temperatures in the middle of the beam spot (i.e. at radius zero): the calculated temperatures are 55.20 and 55.24 K assuming the uniform and the Gaussian beam profiles respectively. For both profiles the beam will penetrate the Xe layer and deposit some energy in the gold substrate. In the case of the Ne beam, the energy loss of the individual ions in the thin Xe layer (1.5 mg/cm^2) is only 1.1 MeV and in the thicker Xe layer (15 mg/cm^2) 62 MeV (using the stopping powers of Anderson and Ziegler [7]). As a 'worst case', though, we consider here the thicker Xe layer and model all the beam to be stopped in this layer at its front surface, thus all the heat has to conduct axially into the substrate.

Thus, to summarize, a model is assumed where all the heat conducts axially through the Xe target and radially through the Au substrate. Also, heating from radiation from the surrounding environment is taken into consideration, as implemented in the code described in [6]. The resulting temperature profile is shown in Fig. 4.

Even though the thermal conductivity of frozen Xe is orders of magnitude lower than that of Au, the Xe layer is too thin for bulk heating taking place if axial conduction to the Au can effectively take place. As can be seen in Fig. 4, the maximum temperature rise is less than 5 K assuming a total energy deposition within the Xe film. If the Xe layer is a well formed 'ice' layer with few imperfections, bulk heating cannot be responsible for Xe loss. It has, however, been reported in [8] that Xe loss on such a frozen layer

Table 1 Some physical properties of Au and Xe in the solid state

	Density (g/cm^3)	Thermal conductivity (W/m/K)	Emissivity	Melting point (K)	Boiling point (K)	References
Au	19.31	327	<0.1	1337.6	3081.2	[9, 10]
Xe	3.64	0.476		161.3	166.1	[9, 10, 12]

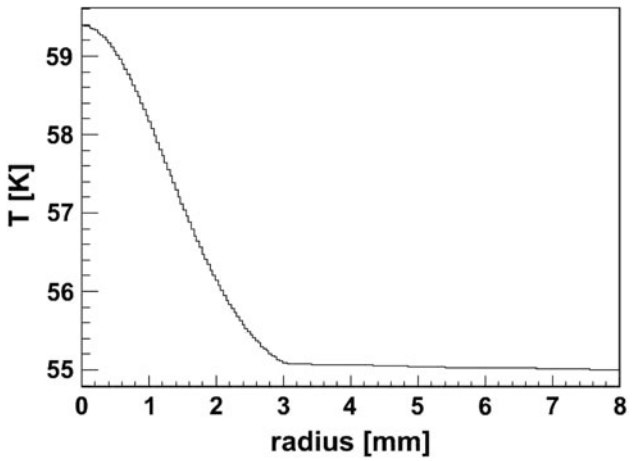

Fig. 4 The radial temperature profile of the maximum temperatures in the Xe layer, assuming a model where the entire thermal load of 90 mW conducts axially through the Xe layer and radially through the Au layer. A Gaussian beam profile truncated at 2× FWHM is assumed (see text)

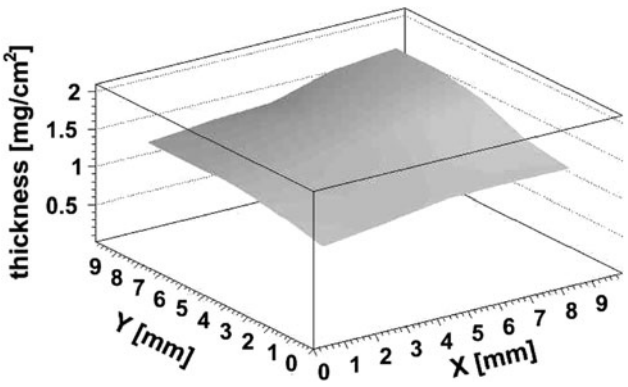

Fig. 5 Thickness profile of the thin Xe target with average thickness 1.47 mg/cm^2

erodes much faster than expected from sputtering only. A mechanism of local heating along an ion track, called 'thermal spiking', has been proposed [8]. Imperfections in the Xe layer, e.g. if some of the layer consists of "snowy" loosely bound clusters, may be an important contributor to Xe erosion due to local heating. The calculation that forms the basis of Fig. 4 also includes a contribution from radiation heating of the target by its warmer environment. The environment was assumed to be at 300 K and all target surfaces were modelled to have a thermal emissivity of $\varepsilon = 0.1$ since it is very unlikely that the emissivity (ε) will ever exceed a value of 0.1 (see e.g. [9]). The resulting increase in the total thermal load by radiation was found to be only about 10 %, spread over a much larger surface than the area irradiated by the beam. Consequently, the effect of radiation heating contributed very little to the target heating.

This is consistent with experience gained in actual experimental runs. Some runs were performed using a thermal shield around the target and some runs without and no significant difference was observed in the Xe erosion rate. The structure of frozen Xe in these conditions is not known precisely. Such structure is more inclined to allow local heating and therefore resulting in an accelerated sublimation rate.

Results and discussions

The thickness measurement was performed without the thermal shield resulting in water and oil deposition. Consequently, the target was contaminated with O and C as indicated by the arrows in Fig. 3. The interstitial contamination is suspected to occur between the cooling of the cold finger and the deposition of Xe while the required temperature is reached. The surface contamination of carbon and interstitial contamination of oxygen appear in a unique peak as a result of the energy loss of protons back scattered through the Xe layer. The interstitial layer has the advantage of separating the Xe peak from the Au continuum, indicated in the spectrum by the arrows. Over long runs the accumulation of oil and water can be detrimental due to substantial contamination with light elements.

The fits of the EBS data are performed with SIMNRA [10] for every individual spectrum recorded on the 2×2 mm^2 samples. Contamination of C and O is deduced from the spectra with hydrogen contamination taken into account for energy loss purposes. The proportion of H to O (H_2O) and C (nCH_2) is estimated to be of 2–1. The gap between Xe and Au and the peaks of interstitial contamination are equally well reproduced, indicating a precise determination of the water and oil deposition on the cold substrate. Calculated Rutherford cross sections were used for Au and Xe whereas experimental cross sections were taken from [11, 12] for proton scattering on C and O, respectively, as the beam energy is substantially above the Coulomb barrier for these light nuclei. The water and oil deposition are measured to be 40 and 60 μg/cm^2/h, respectively, without thermal shield.

In Fig. 5 the resulting thickness of the Xe target is mapped. The target shows good thickness homogeneity over the sampled area with an increase of thickness from bottom left to top right corner. This effect is due to the orientation of the gas feeder closer to the thicker part of the target. The measured average target thickness is (1.47 ± 0.12) mg/cm^2.

Conclusion

In this work, solid Xe films were kept under high vacuum at $T = 55$ K using a cooling system based on solid nitrogen

sublimation. Films between 1.5 and 15 mg/cm^2 were characterized with the EBS technique. The system is simple and compact, contamination from water and oil should be kept low with a dry pump system and a thin thermal shield kept at solid nitrogen temperature. At a temperature of 55 K no contamination from nitrogen or argon is expected under such conditions. To date, two measurements with the AFRODITE γ-ray spectrometer have been carried out: ^{136}Xe (^{22}Ne, 4n) ^{154}Gd at 93 MeV and ^{136}Xe (^{18}O, 4n) ^{150}Sm at 75 MeV, using $\approx$5 mg/cm^2 frozen Xe targets. In both cases the ^{136}Xe was preferably frozen onto the Au substrate. The isotopic purity (99.8 %) of the ^{136}Xe gas and the lack of any other condensates on the target enabled very clean spectra to be produced. Solid Xe targets could have certain advantages in radioactive beam experiments with low erosion because of lower beam intensities. The thickness of the substrate can be adjusted and a large area can be covered.

Acknowledgments One of the authors, P. P., would like to acknowledge Y. Hietter (Canberra, France), P. Paulsen and F. Gonglach (iThemba LABS) for excellent technical support and T. Doyle for invaluable discussions. This work was financially supported by the National Research Foundation (NRF).

References

1. Oganessian Y, Dmitriev SN, Yeremin AV, Aksenov NV, Bozhikov GA, Chepigin VI, Chelnokov ML, Lebedev VYa, Malyshev ON, Petrushkin OV, Shishkin SV, Svirikhin AI, Tereshatov EE, Vostokin GK (2009) Phys Rev C 79:024608
2. Urban W, Bacelar JC, Jongman J, Gast W, Hebbinghaus G, Krämer-Flecken A, Lieder RM, Thoms M, Zell O (1996) Phys Rev C 53:2516
3. Urban W, Rzaca-Urban T, Durell JL, Hess ChP, Pearson CJ, Phillips WR, Varley BJ, Vermeer WJ, Vieu Ch, Dionisio JS, Pautrat M, Bacelar JC (1996) Phys Rev 54:2264
4. Jongman JR, Urban W, Bacelar SJC, van Pol J, Nyberg J, Sletten G, Dionisio JS, Vieu C, Lagrange JM, Pautrat M (1995) Nucl Phys A591:244–264
5. Lipoglavšek M, Likar A, Vencelj M, Vidmar T, Bark RA, Gueorguieva E, Komati F, Lawrie JJ, Maliage SM, Mullins SM, Murray SHT (2006) Nucl Instrum Methods A 557:523–527
6. Steyn GF, Nortier FM, Mills SJ (1990) Nucl Instrum Methods A 292:35–44
7. Anderson HH, Ziegler JF (1977) The stopping and ranges of ions in matter. Pergamon, New York
8. Ollerhead RW, Tiger JB, Davies JA, L'Ecuyer J, Haugen HK, Matsunami N (1980) Radiat Eff 49:203
9. Aprile E, Bolotnikov AE, Bolozdynya AI, Doke T (2006) Front matter. In Noble gas detectors, Wiley-VCH Verlag GmbH & Co. KGaA, Weinheim, Germany. ISBN 3527609636
10. Mayer M (1997) SIMNRA user's guide, Report IPP 9/113. Max-Planck-Institut für Plasmaphysik, Garching. http://home.rzg.mpg.de/~mam/. Accessed 9 July 2013
11. Mazzoni S, Chiari M, Giuntini L, Mando PA, Taccetti N (1998) Nucl Instrum Methods B 136–138:86–90
12. Gurbich AF (1997) Nucl Instrum Methods B 129:311